Bulgarian Chemical Communications, Volume 50, Special Issue L (pp. 180 –187) 2018

Safranin-O dye removal from aqueous solution using super-absorbent lignin nanoparticle/polyacrylic acid hydrogel

KH. Didehban*, S. A. Mirshokraie, J. Azimvand

Department of Chemistry, Payame Noor University, Tehran, Iran

Submitted March 24, 2016; Accepted August 8, 2016

Alkali lignin (AL) modified by ethylene glycol and lignin nanoparticles (LN) was prepared through the acid precipitation technology. Lignin nanoparticle/polyacrylic acid (LN/PAA) hydrogel was prepared using copolymerization reactions.

LN and LN/PAA hydrogel were investigated using GPC, SEM, FT-IR spectroscopy, and TGA-DTG analysis. The sizes of the nanoparticles were assessed using DLS.

LN/PAA hydrogel was used to remove Safranin-O from an aqueous Solution. The optimal conditions for absorption provided at pH 7, an initial concentration of dye of 1.5 gr.L^{-1}, and an adsorbent dosage of 0.1 gr. Also, the optimal time for LN and LN/PAA hydrogel were 100 min and 450 min, respectively. Both absorbent LN and LN/PAA hydrogel showed good agreement with the Langmuir isotherm. The maximum absorption capacities of LN and LN/PAA hydrogel were determined to be 100 mg.gr^{-1} and 1666.6 mg.gr^{-1}, respectively. Both absorbent LN and LN/PAA hydrogel follow the pseudo-second kinetic model and the intraparticle diffusion model.

Keywords: Lignin, Nanoparticles, Ethylene glycol, Polyacrylic acid, Safranin-O, Hydrogel

INTRODUCTION

Safranin-O dye is highly soluble in water and is nonvolatile. It is red in color and is a cationic dye of the imine group. Safranin-O is dangerous and toxic [1].

Adsorption processes are physical processes that have advantages compared to other waste technologies; they are low cost, accessible, and capable of treating dye in high concentrations. A variety of natural and synthetic absorbents are used to bleach dyes; natural adsorbents are environmentally friendly, are low cost, have a high absorption capacity, lack toxicity, and cause few problems in the final desorption phase [2].

After cellulose, lignin is the second most abundant natural polymer; it consists ofphenylpropane structural units with carbon–carbon and ether connections. Lignin is an amorphous and super complex structure that has yet to be fully investigated [3].

Hydrogels are three-dimensional structures with linear polymer chains that have covalent bonds. Nanocomposite hydrogels are network structures of hydrophilic homopolymers or copolymers. Some hydrogels are not used widely because of their low stability, high production cost, and toxicity. Therefore, the use of natural materials in nanocomposite hydrogel is very functional due to their easy operation, low power consumption, easy maintenance, high absorption capacity, and high performance [4]. Luo et al., in 2015, evaluated the chemical properties of nanocomposite hydrogels and prepared isopropyl acrylamide/alkali lignin [5]. In 2011, Ma et al. prepared a cellulose/acrylic acid copolymer by the copolymerization of radicals; the absorption capacity of methylene blue and the rate of swelling were determined to be 2,197 mg.gr^{-1} and 7,32%, respectively [6].

The purpose of this research was to prepare LN/PAA hydrogel for the removal of Safranin-O. In addition, the pH, adsorbent dosage, dye concentration, and contact time were studied as factors in the absorption process. Further, pseudo-first order, pseudo-second order, and intraparticle diffusion were investigated in the Langmuir, Freundlich, and Temkin models to evaluate the absorption processes.

MATERIALS AND METHODS

Materials

AL was prepared by the acidification of black liquor obtained from the Pars Khuzestan paper factory in Iran. Safranin-O dye (99.5%), sodium hydroxide (99%), hydrochloric acid (wt% 36), and ethylene glycol (98%), potassium persulfate, N,N′-Methylenebis(acrylamide) (98%), and acrylic acid purchased from Merck in Germany. Ethanol (99.9%) was prepared by Bidestan in Iran. The chemical structure and features of the Safranin-O dye are shown in Table 1 [7].

---

* To whom all correspondence should be sent:
E-mail: Didehban95@gmail.com

Table 1. Chemical and physical characteristics of the Safranin-O dye [7]

C.I. name	Safranin-O
C.I. number	50240
Common name	Basic red 2
Other name	Safranin-T, Basic red 2
Class	Safranin
Ionization	Basic
Aqueous solubility (%)	5.45
Colour	Red
Absorption maximum (nm)	517
Chemical formula	C20H19N4Cl
Formula weight (g/mol)	350.85
structure	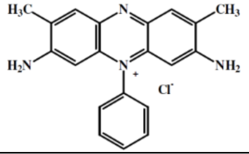

Devices

Fourier transform infrared spectroscopy (FT-IR) was used to determine the chemical structures of the compounds in the range of 400 to 4,000 cm^{-1} using a Tensor 27 FT-IR spectrophotometer made by Brucker in Germany. In order to determine the amount of dye absorption, Safranin-O dye was used. To determine the amount of ultraviolet-visible absorption, a Model M350 Double Beam Spectrophotometer was used (UK). The pH was determined using a Model Metrohom 827 pH meter. In order to study structural changes in the synthesis of compounds as well as heat resistance up to 500°C, a thermogravimetric analysis (TGA-DTG) device (Model Perkin Elemr) was used (UK). In addition, a Zetasizer PSS0012-22 (Malvrn) made in USA was used for dynamic light scattering (DLS), and scanning electron microscope (SEM) device (Model LEO 1455VP) made in UK, was used in order to determine the particle size and morphology of the surface of the absorbent. Gel permeation chromatography (GPC) was performed with a Shimadzu 6-A made in USA, to determine the molecular weight of the AL.

Preparation of alkaline lignin

To precipitate the AL, acidic black liquor from a pulp and paper factory in Khuzestan was placed in 0.1 N of hydrochloric acid in a pH range of 2.5–3. The impure lignin precipitate sediment was centrifuged and isolated. The sediment was washed with distilled water until the filter effluent reached a pH of about 7. In order to purify, lignin was dissolved in relatively warm ethanol (50–60°C). Ethanol-soluble fractions were separated by filtration, and the solid residue was discarded. The bulk of the ethanol (75%) in the evaporator was evaporated at low pressure. Distilled water was poured on the remaining solution and the sediment of lignin in a colloidal form [8]. The molecular weight (M_w) and polydispersity index (PDI) of the AL obtained 2530 $gr.mol^{-1}$ and 1.65, respectively, using gel permeation chromatography.

Preparation of lignin nanoparticles

AL (0.28 gr) was dissolved in 50 ml of polyethylene glycol (wt% 0.56) and was stirred for 2 h at a temperature of 40° C. Then, it was filtered with 0.4-μm filters for purification. Next, hydrochloric acid 0.25 M was slowly dropped in 45 ml of the filtered solution at a pH of 4. The Lignin nanoparticles were formed in this solution [9].

Preparation of the LN/PAA hydrogel

First, 0.38 ml of acrylic acid monomer and 50 ml of distilled water were poured into a three-neck round-bottom flask equipped with a reflux condenser and were stirred until completely dissolved by the magnetic stirrer. Then, 0.25 gr of LN was added; using a sodium hydroxide solution (wt% 10), the pH of the solution was increased to 11. The reaction temperature was adjusted to 60°C, and the solution was stirred for 30 min. Next, 0.1 gr of potassium persulfate and 1.9 gr N,N′-Methylenebis(acrylamide) was added to the contents of the flask as the initiator and nitrogen gas flowed in the flask for 15 min, to eliminate the damaging effects of oxygen in the reaction. Reflux was performed at 60 °C for 30 min. In order to stop the reaction, the reflux was stopped, and the flask was cooled at room temperature. After 4 h, the hydrogel was formed [10]. The mechanisms used for the preparation of the LN/PAA hydrogel are presented in Figure 1.

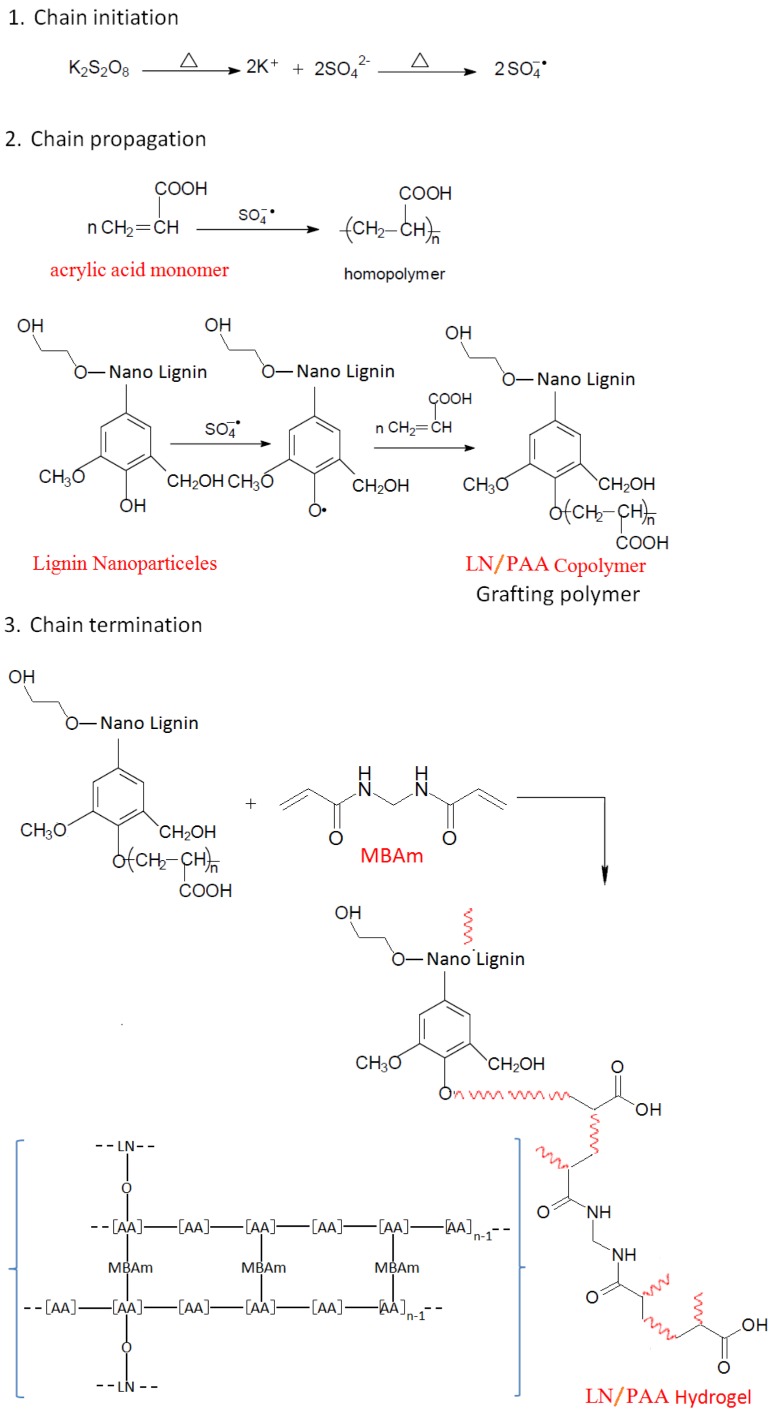

Fig. 1. Mechanisms used to prepare the LN/PAA hydrogel.

Safranin-O dye absorption

A stock solution with a concentration of 2 gr.L^{-1} was prepared and maintained at a temperature of 4°C. All experiments were carried out with 100 ml of dye at a temperature of 25°C on a shaker at 70 rpm. The samples were filtered after each step to measure the concentration of the dye, and the absorption rate was determined using ultraviolet-visible absorption spectroscopy at a wavelength of 517 nm. Each sample was tested three times, and the averages were recorded. The amount of dye adsorbed at equilibrium (qe(mg.gr^{-1})) and the dye removal efficiency (R%) were determined using equations (1) and (2), respectively [11].

$$q_e = (C_0 - C_e)/M \qquad (1)$$

$$\% = 100(C_0 - C_e)/C_0 \qquad (2)$$

C_0 and C_e represent the initial and final concentrations of dye in the solution (mg.L^{-1}), respectively, V is the volume of the solution (L), M is the adsorbent mass (gr), and q_e is the amount of dye adsorbed at equilibrium (mg.gr^{-1}).

Isoelectric range

The point zero charge (pH_{pzc}) characteristic of LN and LN/PAA hydrogel was determined using the solid addition method [12]. The experiment was conducted in a series of 100 mL flasks with glass-stoppered. Each flask was filled with 20 mL of potassium nitrate 0.1M solutions of different initial Ph values (pH_0) and 0.20 g of LN or LN/PAA hydrogel. The pH values of the KNO_3 solutions were adjusted 2-10 with sodium hydroxide 0.1M and diluted hydrochloric acid. The suspensions were then sealed and shaken for 24h at 100 rpm and 24°C. The final Ph values (pH_f) of the supernatant liquid were noted. The difference $\Delta pH(pH_0 - pH_F)$ between the initial and final pH values was plotted against pH_0. The point of intersection of the resulting curve with the abscissa gave the pH_{PZC}.

RESULTS

Determining lignin nanoparticle size using dynamic light scattering

The particle size distribution of lignin nanoparticles at a pH of 4, as a function of the percentage of nanoparticles, is presented in Figure 1. The LN size at a pH of 4 was estimated to be between 40 nm and 60 nm, and the average diameter of the nanoparticles was determined to be 52.7 nm.

Morphology of alkali lignin and lignin nanoparticles

In order to study the morphology and approximate particle size of AL, LN and LN/PAA hydrogel, a scanning electron microscope was used. The AL and LN morphologies, before and after the adsorption of Safranin-O, are shown in Figure 2. AL macromolecules have homogeneous and interconnected particles that are relatively uniform and flat. LN have an average diameter of less than 80 nm and highly porous surfaces. The matrix surface has a honeycomb structure with a relatively uniform dispersion.

FT-IR spectra

The FT-IR spectra of PAA, AL, LN, and LN/PAA hydrogel are shown in Figure 3. The FT-IR spectra of AL and LN are very similar to each other. No change was seen in the chemical structure of AL in the process of creating nanoparticles. The weak peak at 1,709 cm^{-1} shows the good vibration of Carbonyl bonds in the carboxylic acid groups. The peak at 1,315 cm^{-1} in the LN shows the stretching vibration in connecting syringyl (S) and guaiacyl (G), which occurred as a result of nanoparticles formation. In AL compound, The peak at the 3,405 cm^{-1} area relates to the vibration of -OH bonds, which, in LN compound due to connection with the ethylene glycol, moved to 3,394 cm^{-1} and increased in intensity. The stretching vibration of amide carbonyl groups in the 1,628 cm^{-1} area indicates the presence of crosslinking N,N'-methylene-bisacrylamide in the LN/PAA hydrogel. In the LN/PAA hydrogel, the carbonyl group in the carboxylic acid transferred from the 1,709 cm^{-1} area to the 1,716 cm^{-1} area as a result of copolymerization. Thus, PAA chains containing carboxylic acid groups was network to LN in the LN/PAA hydrogel.

Thermal stability

The thermogravimetric analysis (TGA) and differential thermogravimetric (DTG) spectra of PAA, LN and, LN/PAA hydrogel are shown in Figure 4. The weight loss of LN occurred in two stages. The first was attributed to the evaporation of water and the second, which was attributed to the breaking of the syringyl, guaiacyl, and p-hydroxyphenyl polymer units in the LN. But weight loss in the PAA samples and LN/PAA hydrogel was done in three stages. The first, which was attributed to the evaporation of water contained in the compounds. The second, which was attributed to the decomposition of carboxylic acids and breaking of the crosslinker in the hydrogel. Also, The third, which was attributed to the breaking of the main chain in the PAA and breaking of the syringyl, guaiacyl, and p-hydroxyphenyl polymer units in the LN/PAA hydrogel

.

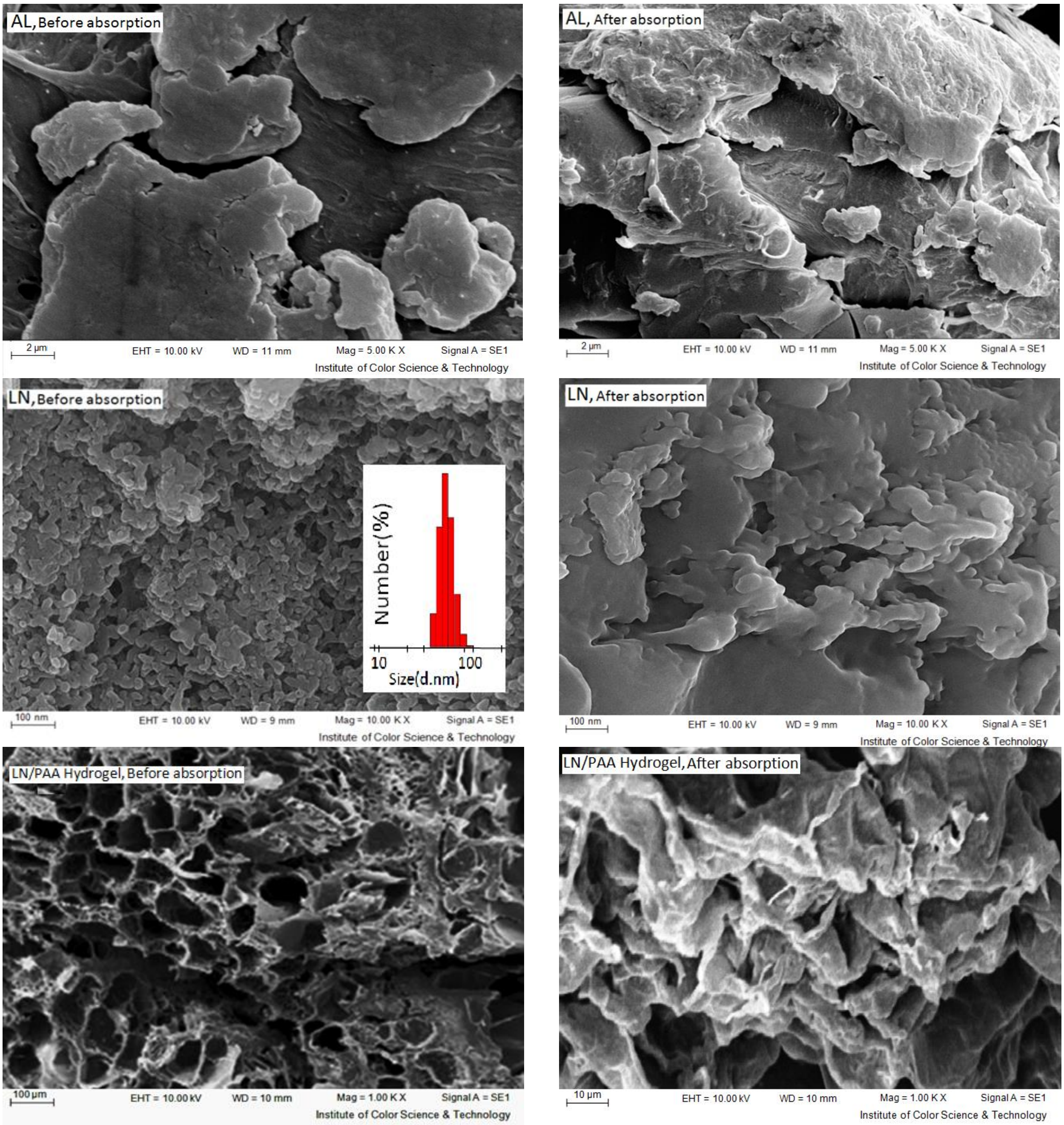

Fig. 2. SEM images of AL, LN and LN/PAA hydrogel before and after the absorption of Safranin-O dye.

In the LN/PAA hydrogel, increasing the temperature to 341°C resulted in the carboxylic acid groups in the PAA breaking and crosslinker bond decomposition, preventing heat transfer to the main structure of the LN. Break the main chains in the LN and LN/PAA hydrogel begins at temperature 146°C and 341°C, respectively, which has increased 195°C in the LN/PAA hydrogel. The results show more structural changes in the LN/PAA hydrogel compared to in the LN due to copolymerization with polyacrylic acid and crosslinking formation.

Factors that affect absorption

Effect of initial pH. The optimal pH was investigated. According to the stability of LN/PAA hydrogel, the absorption of Safranin-O dye was evaluated at a pH range of 3–10.

The isoelectric points (pH_{PZC}) of the LN and LN/PAA hydrogel were 5.6 and 5.5, respectively. The pH_{PZC} decrease in the LN/PAA hydrogel was attributed to the increased K_a in the AA monomers; as a result, acidic hydrogen released in a lower pH. A decrease in pH from pH_{PZC} to 2 reduced the absorption capacity and the percentage of dye removal; this is because, by reducing the pH, the concentration of H^+ increased, so many $-NH_2$ functional groups were protonated on the dyes quantitatively and were unable to create hydrogen bonds.

At pH_{PZC}, the compounds had no electric charge; however, at $pH > pH_{PZC}$, the electrical charge was negative due to the loss of acidic hydrogen in the carboxylic acid groups of the LN and LN/PAA hydrogel. By introducing electrostatic attraction with the Safranin-O dye, the absorption capacity and percentage of dye removal increased. In a pH range of 5–6, the adsorption capacity and percentage of dye removal increased dramatically. The absorption capacities of LN and LN/PAA hydrogel at a pH of 7 were 90 mg.g^{-1} and 941 mg.g^{-1}, respectively. The adsorption data at a pH of 10 demonstrates the significant effect of carboxylic acid groups on the creation of electrostatic attraction in the process of absorption.

Effect of adsorbent dosage. The effect of adsorbent dosage on the adsorption of Safranin-O dye was investigated. By increasing the amount of absorption, the absorption capacity reduced slightly; this is because, with low amounts of absorbent, there is more competition between dye molecules to connect to the absorbent. Thus, the absorption capacities of the LN and LN/PAA hydrogel in the use of 0.02 gr of absorbent were 210 mg.g^{-1} and 1320 mg.g^{-1}, respectively. By increasing the amount of absorbent to 0.1 gr, the absorption capacities of the LN and LN/PAA hydrogel reduced to 91.9 mg.g^{-1} and 995 mg.g^{-1}, respectively.

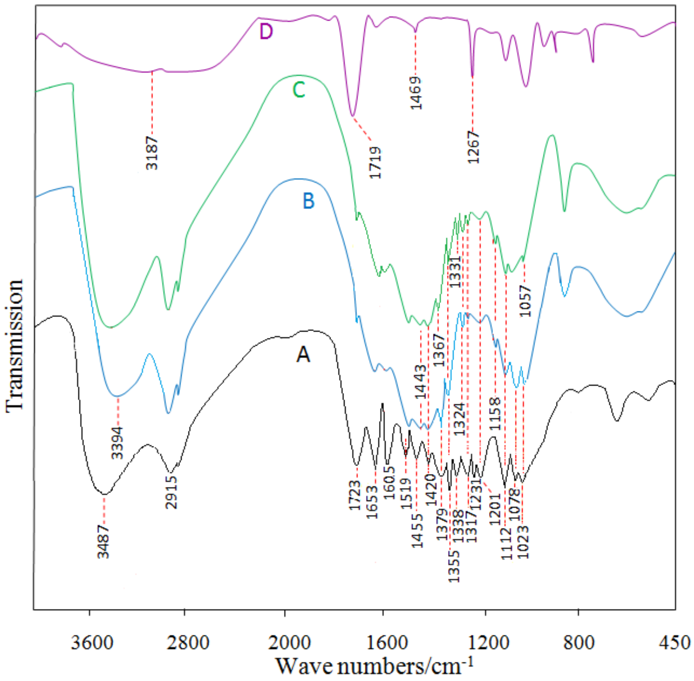

Fig. 3. FT-IR spectra of LN/PAA hydrogel (A), LN (B), AL (C) and PAA(D).

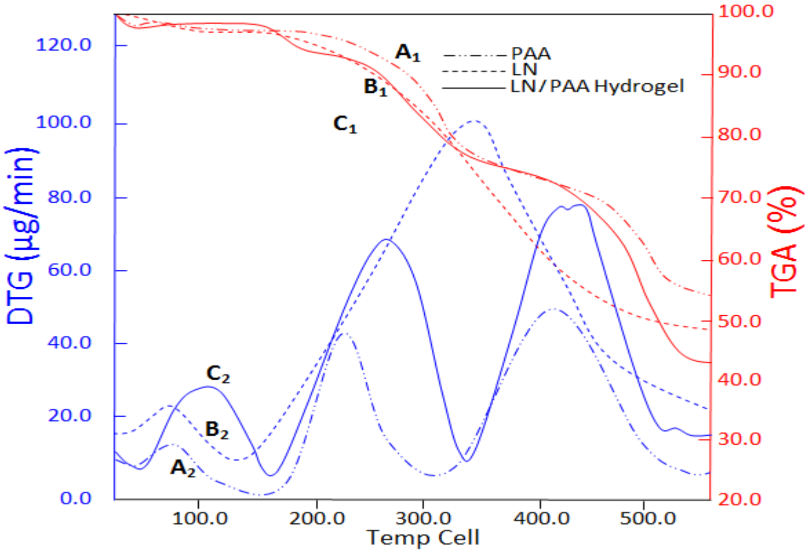

Fig. 4. TGA and DTG curves in the PAA (A_1 and A_2), LN (B_1 and B_2) and LN/PAA hydrogel (C_1 and C_2)

Effect of contact time. The effect of contact time on Safranin-O dye absorption was evaluated. The adsorption capacity and percentage of Safranin-O dye removal for both LN and LN/PAA hydrogel was initially rapid; after about 100 min for LN Compound and 450 min for LN/PAA hydrogel , they reached equilibrium and remained almost constant. Therefore, the optimal times for LN and LN/PAA hydrogel were determined to be 100 min and 225 min, respectively. At optimal time, the removal capacities of LN and LN/PAA hydrogel were 99.2 $mg.g^{-1}$ and 1060 $mg.g^{-1}$, respectively.

Effect of initial dye concentration. The effect of initial dye concentration on the absorption capacity and percentage of dye removal was investigated using adsorbent LN and LN/PAA hydrogel. With increased initial dye concentrations, a greater amount of dye interacts with the surface of the absorbent, thereby increasing the absorption capacity. The absorption capacities, at a maximum concentration of 1.5 $gr.L^{-1}$ of LN and LN/PAA hydrogel absorbent, were 91.9 $mg.g^{-1}$ and 1060 $mg.g^{-1}$, respectively.

Adsorption isotherms. Adsorption isotherms provide equations to describe the adsorption equilibrium between solid and fluid phases. The Langmuir and Freundlich equations are shown in equations (3) and (4), respectively [13].

$$\frac{C_e}{q_e} = 1/(q_{max}.K_L) + (\frac{C_e}{q_{max}} \qquad (3)$$

$$\mathrm{Ln}\, q_e = \mathrm{Ln}\, K_F + 1/n(\mathrm{Ln}\, C_e) \qquad (4)$$

$K_L(L.gr^{-1})$ represents the Langmuir isotherm constant, q_{max} $(mg.gr^{-1})$ is the maximum absorption capacity, n and $K_F(mg.L^{-1})$ are Freundlich isotherm constants, and $C_e(mg.L^{-1})$ is the concentration of adsorbates, after reaching equilibrium in the liquid phase and the q_e $(mg.gr^{-1})$ amount of adsorbates in the unit mass of the absorbent. K_F represents the absorption capacity, and 1/n represents the adsorption intensity.

An essential characteristic of the Langmuir isotherm is a constant and dimensionless parameter called R_L, which can be obtained from equation (5) [13].

$$R_L = 1/(1 + K_L.C_0) \qquad (5)$$

C_0 $(mg.L^{-1})$ represents the initial dye concentration in the solution.

The Temkin isotherm is linear and can be determined by equation (6) [13].

$$q_e= B_t.\mathrm{Ln}\, K_t+ B_t.\, \mathrm{Ln}\, C_e \qquad (6)$$

Using the curve q_e in Ln C_e, B_t and K_t were determined by the slope and intercept of the curve.

Evaluation of the Langmuir, Freundlich, and Temkin isotherm models

The Langmuir, Freundlich, and Temkin isotherm models Models were examined, and their data are shown in Table 2. The R_L data in the Langmuir model and 1/n in the Freundlich model for both the LN and LN/PAA absorbents are between 0 and 1; the Safranin-O dye absorption of both the LN and LN/PAA hydrogel was assessed desirable using the Langmuir and Freundlich models. The R_2 greater in the both the LN and LN/PAA hydrogel showed dye absorption followed of the Langmuir isotherm. The maximum adsorption capacity of LN was 100 $mg.g^{-1}$ and that of LN/PAA hydrogel was 1666.6 $mg.gr^{-1}$ in the Langmuir model, both of which are close to the experimental values. The high absorption capacity of the LN/PAA hydrogel was attributed to the quantitative increase in carboxylic acid groups in the polymer chain of the AA connected to the phenoxy radicals in the LN during polymerization.

Table 2. Effect of the Langmuir isotherm, Freundlich isotherm, and Temkin isotherm on Safranin-O dye adsorption (dye concentration = 1.5 $gr.L^{-1}$, pH = 7, adsorbent dose = 0.1 gr, contact time = 100 min (for LN) and 450 min (for LN/PAA hydrogel)).

Absorbent type	Temp (°C)	Langmuier isotherm				Freundlich isotherm				Temkin isotherm		
		R^2	$q_{e\,max}$ $(mg.gr^{-1})$	K_L $(L.g^{-1})$	R_L	R^2	1/n	n	K_F $(L.mg^{-1})$	R^2	B_t	K_t
LN	25±2	0.999	100	0.012	0.052	0.68	0.11	8.96	40.52	0.69	9.2	14.29
LN/PAA Hydrogel		0.981	1666.6	0.0001	0.87	0.68	0.131	7.51	627.09	0.78	169.8	13.06

Absorption kinetics

Absorption kinetics were studied to determine the factors that influence the rate of absorption. The linear pseudo-first-order kinetic model is shown in equation (7) [14].

$$\mathrm{Ln}(q_e - q_t) = \mathrm{Ln}(q_e) - (K_1 t) \qquad (7)$$

The linear pseudo-second-order kinetic model is shown in equation (8) [14].

q_e $(mg.gr^{-1})$ represents the amount of dye adsorbed at equilibrium, q_t $(mg.gr^{-1})$ shows the amount of dye adsorbed at time t, and $K_1(min^{-1})$ represents constant first-order kinetics at equilibrium.

$$\frac{t}{q_t} = \frac{1}{k_2.q_e^2} + (\frac{t}{q_e}) \qquad (8)$$

K_2(gr.mg^{-1}.min^{-1}) represents constant first-order kinetics at equilibrium.

The intraparticle diffusion model is presented in equation 9 [14].

$$q_t = K_p.t^{1/2}+C \quad (9)$$

K_p (mg.gr^{-1}.min$^{-1/2}$) is the intraparticle diffusion constant and C (mg.gr^{-1}) Intraparticle diffusion constant. Using the curve q_t in $t^{1/2}$, K_p and C were determined.

Evaluation of pseudo-first- order, pseudo-second-order, and intraparticle diffusion kinetic models

K ‘q_e and R^2 in the pseudo-first-order and pseudo-second-order kinetic models and Kp and C in the intraparticle diffusion model were examined, and their data are shown in Table 3. The correlation coefficients (R_2) in the pseudo-second-order and intraparticle diffusion kinetic models are similar and are greater than the correlation coefficient in the pseudo-first-order kinetic model. Therefore, the bleaching process can be described by both pseudo-second-order and intraparticle diffusion models.

In the pseudo-second-order kinetic model, the absorption capacities of LN and LN/PAA hydrogel were 99 mg.gr^{-1} and 909.09 mg.gr^{-1}, respectively, in the computational results and 92 mg.gr^{-1} and 1060 mg.gr^{-1}, respectively, in the experimental results. The proximity of the experimental and theoretical results show that the pseudo-second-order kinetic model is appropriate to determine Safranin-O dye adsorption in LN and LN/PAA hydrogel.

Table 3. Pseudo-first-order, pseudo-second-order, and intraparticle diffusion kinetic models for BR2 dye adsorption (dye concentration = 1.5 gr.L^{-1}, pH = 7, adsorbent dose = 0.1 gr, contact time = 100 min (for LN) and 450 min (for LN/PAA hydrogel)).

Absorbent rtype	t° (°C)	$(q_e)_{Exp}$ (mg.g^{-1})	Pseudo-first –order model			Pseudo-second -order model			intraparticle diffusion model		
			R^2	$(q_e)_{Cal}$ (mg.g^{-1})	K_1 (min^{-1})	R^2	$(q_e)_{Cal}$ (mg.g^{-1})	K_2 (min^{-1})	R^2	Kp	
LN	25±2	92	0.84	42.5	0.033	0.999	99	0.0012	0.99	3.2	60.13
LN/PAA Hydrogel		1060	0.86	601.8	0.005	0.992	909.09	0.000057	0.97	21.7	512.29

CONCLUSION

This study was conducted to assess the efficacy of LN/PAA hydrogel Nanocomposites as cheap Superabsorbent that are environmentally friendly in the removal of cationic Safranin-O from aqueous solutions. The results showed that the absorption capacity in LN/PAA hydrogel increased than the LN to almost 16.5-fold. Adding polar groups of -COOH to the structure of natural absorbents is an effective method to absorb Safranin-O dye; by increasing electrostatic attraction and hydrogen bonding, the absorption capacity and percentage of dye removal also increase.

Absorption using pseudo-second-order and intraparticle diffusion kinetic models for LN and LN/PAA hydrogel absorbents occurs according to the principles of two-stage absorption kinetics. In the first stage, the dye removal rate is increased by adsorption; in the second stage, the dye removal rate is decreased due to the influence of the porous surface.

Thus, LN/PAA hydrogel achieved a suitable absorption capacity and compatibility with the environment; thus, they are suitable for the removal of wastewater containing Safranin-O dye.

REFERENCES

1. R. Gong, M. Li, C. Yang, Y. Sun, J. Chen, *J. Hazard. Materials*, **121**, 247 (2005).
2. D. Mohan, K. P. Singh, G. Singh, G. Singh, K. Kumar, *Ind. Eng. Chem. Res*., **41**, 3688 (2002).
3. S. Hu, Y. L. Hsieh, *Carbohydr. Polym.*, **131**, 134 (2015).
4. W.F. Lee, L.G. Yang, *J. Appl. Polym. Sci.*, **92**, 3422 (2004).

5 H. Luo, S. Ren, G. Fang, G. Jiang, *BioResources*, **10**, 3507 (2015).

6. Y. Zhou, S. Fu, H. Liu, H. Zhan, *Polym. Eng. Sci.*, **51**, 2417 (2011).
7. A. Hamidi, S. Jedari, *Sharif. Civ. Eng. J*. **29**, 29 (2011).
8. K. Gupta, S. Mohanty, S. K. Nayak, *Mater. Focus*, **3**, 444 (2014).
9. C. Frangville, M. Rutkevičius, A. P. Richter, O. D. Velev, S.D. Stoyanov, V.N. Paunov, *Chemphyschem*., **13**, 4235 (2012).
10. Y. Sun,Y. Ma, G. Fang, S. Li, Y. Fu, *Bioresources*, **11**, 5731 (2016).
11. J. M. Fanchiang, D. H. Tseng, *Chemosphere*, **77**, 214 (2009).
12. Y. Tang, Y. Zeng, T. Hua, Q. Zhou, Y. Peng, *J. Environ. Chem. Eng*., **4** , 2900 (2016).
13. Y. Niu, R. Qu, C. Sun, C. Wang, H. Chen, C. Ji, Y. Zhang, X. Shao, F. Bu, *J. Hazard. Materials*, **244**, 276 (2013).
14. A. Gil, F. C. C. Assis, S. Albeniz, S. A. Korili, *Chem. Eng. J.*,**168**,1032 (2011).